

**Tunneling, Mining and Rock Slope Analyses using Q-parameters and JRC-JCS parameters, in place of H-B and the Repeating GSI**

3 Nick Barton

4 Nick Barton & Associates, Oslo, Norway  
5 nickrbarton@hotmail.com

**Abstract.** This invited opening lecture will address various aspects of the ISAMET-2026 conference topics. From Theme 1 *Mining*, these sub-themes will be partially illustrated: Rock Mechanics and Ground Control, Design of Surface and Underground Mines, Advances in Drilling and Blasting. From Theme 3 *Tunneling and Excavation*, the following will be partially illustrated: Tunneling in Different (and Difficult) Ground Conditions, Advances in Urban Tunneling, Tunnel Design and Planning and Underground Spaces and Caverns. As promised by the title of the paper, use will be made of methods developed by the author such as the Q-system parameters. These will sometimes be utilized in pairs for special purposes:  $J_n/J_r$  for predicting overbreak,  $J_r/J_a$  for predicting frictional strength. The whole six-parameter Q-formula is used when predicting tunnel and cavern single shell (NMT) reinforcement and support, both for mining and civil constructions. This will be contrasted to double-shell NATM. A truncated version of Q termed Q', just  $RQD/J_n \times J_r/J_a$  is utilized for mine stope dimensioning using hydraulic radius rather than span or height. When relating Q to the deformation modulus and P-wave velocity, *both* of which are depth- or stress-dependent, the normalized form  $Q_c = Q \times UCS/100$  is used. This gives an almost eight-orders of magnitude scale of rock mass quality, far closer to the geological reality than the two '5 to 95' (approx.) methods of RMR and GSI. Although the latter two are very widely used it appears from recent international review that the Q-system is the most widely used in underground civil and mining. GSI is most used for surface and slope work. GSI together with Hoek-Brown formulations for rock mass shear strength will be contrasted with numerical modelling that is based on discontinuum rather than continuum modelling. For this purpose the au-

thor's joint strength parameters: JRC concerning roughness and JCS concerning joint wall strength will be used. They are used in distinct element models like UDEC-BB. Both tunnel models and slope models will be addressed. GSI will be criticized for its remarkable repetition in the H-B equations, which suggests unreliable strength estimates.

**Keywords:** Tunnels, Caverns, Q-value, Collapses, Slopes, Joints

## 1 Introduction

For various reasons that originated when in Imperial College long ago, the author started his immersion in rock mechanics with the development of tension fractures in brittle model materials, followed by development of sets of tension fractures, and then intersecting sets, so that '2D' open-pit slope models could be formed 'efficiently' with 40,000 blocks. This was followed ten years later by tunnel and cavern models with 20,000 blocks, when working at NGI in Oslo. This physical model immersion had two advantages. The shear strength of the fractures needed to be understood and a much larger number of blocks could be modelled than in available computer codes, such as the early Goodman solution with joint elements. This was before Cundall and UDEC.

A peak strength equation involving the following variables:  $\sigma_c$ , UCS and  $30^\circ$  (for  $\phi_b$ ) was developed in 1967, but subsequently broadened to the familiar JRC, JCS and  $\phi_r$  parameters by 1977, after detailed experimentation with 130 naturally jointed samples in seven different rock types. [1] Barton and Choubey, 1977. Following the outstanding research of Bandis on scale effects, which is summarized in [2] Bandis et al. 1981, these parameters could later be incorporated in UDEC in the form UDEC-BB. The date was 1985.

Such discrete element models, including Cundall's and Itasca's 3DEC provided the most realistic simulations of excavations in jointed rock that were available up to that time. As this new style of realistic modelling for tunnels, slopes and parts of mines was freeing us from continuum FEM modelling, it was for the author and perhaps many others a surprise when so many adopted the Rocscience continuum code Phase 2 and later RS2 with the newly developed GSI and Hoek-Brown equations for the assumed shear strength of rock masses. Since this was based on the earlier empirical equation for the strength of *intact rock* it seems that users had confidence, despite the fact that discrete jointing and faulting had disappeared. This was, and still is, an alarming trend. Figure 1 can be used to illustrate why the representation of jointing, even with 2D limitations, is likely to be important. Was saving money and effort so important? As will be shown later, we need to treat GSI-based solutions with the modified H-B equations for rock masses with great caution.

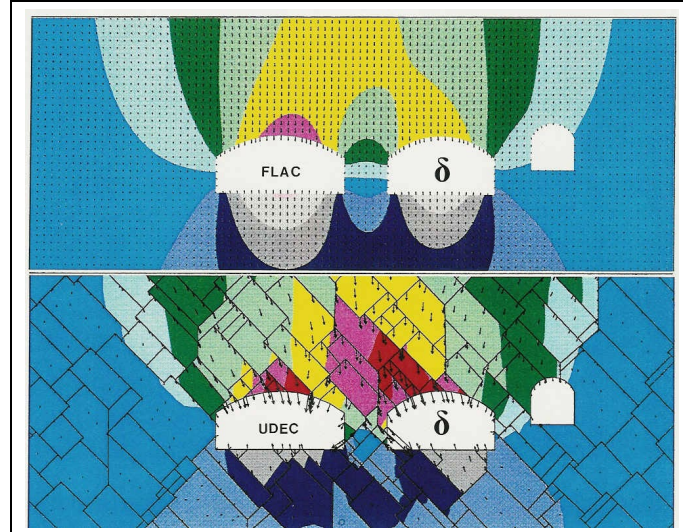


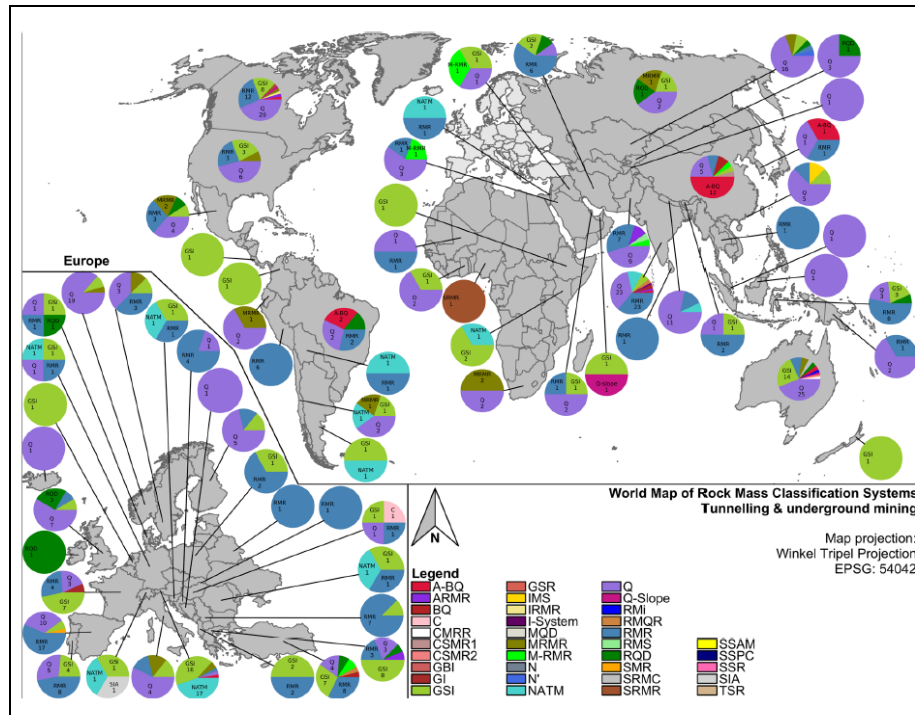
**Fig. 1.** The same geometry and deformation modulus. Which model represents something of value and interest? (Priv. comm. Lise Backer, NGI, 1990).

The development of the shear strength criterion that utilized the rock joint parameters JRC, JCS and  $\phi_b$  (later  $\phi_r$ ) preceded the ‘accidental’ development of the Q-system by several years. The latter had simpler terms for joint and clay-filled joint properties, namely Jr and Ja. As we shall see during the development of his paper / lecture, Jr and Ja will be used when JRC and JCS do not adequately provide answers for the specific cases of clay-coated or clay-filled joints. Each of these sets of strength parameters are very different to the attempted representation of rock mass properties by the two-parameter GSI used by so many at present, for instance when modelling jointed and faulted rock-slopes as continua. Clearly this short-cut has serious limitations.

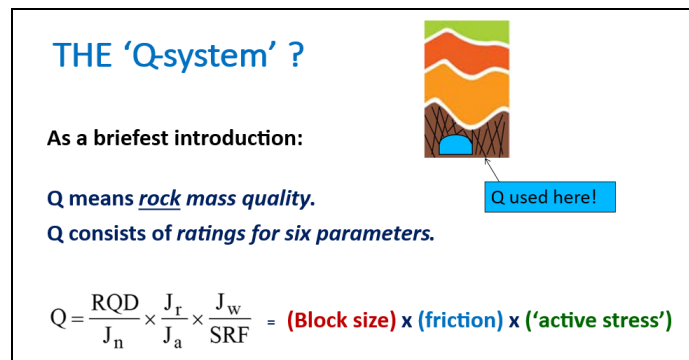
## 2 The Q-system and its Various Uses in Tunneling and Mining.

The Q-system was developed by the author due to a question received by NGI from our Norwegian State Power Board (Statkraft today). ‘Why do our underground hydropower machine and transformer halls suffer such a range of deformation?’ The question was passed to the author. It took six months to send an answer as RQD and adjectives about rock mass quality, plus depth, stress, span, height, support (shotcrete and rock bolts) needed to be integrated into a quantified (Q) ‘system’. Initial scepticism from Trondheim in particular, gradually reduced, and it became the chosen method for selecting tunnel and cavern support, perhaps outside the official Norway before back home in

98 Norway. Figure 2 shows a recent international multi-country review by [3]  
 99 Erharter et al. 2024. 'Purple' (Q) is widespread for underground application.  
 100



101 **Fig. 2.** The international distribution of rock mass classification systems for  
 102 underground application (tunneling and underground mining). India indicates  
 103 about equal use of RMR (blue) and Q (purple). For surface use, GSI (green)  
 104 dominates strongly internationally. Erharter et al. 2024. Figure 3 summarizes  
 105 the logic of Q: relative block-size x inter-block friction, and adjustments for  
 106 faults, stress/strength, swelling, squeezing, each as applicable.  
 107



108 **Fig. 3.** The basic structure of the Q-system and its application in jointed-rock.

## 2.1 Tunnel and Cavern Support based on Q is termed NMT

The Q-system was based on the detailed analysis and application of case records which were synthesized using the gradually developed parameters  $J_n$ ,  $J_r$ ,  $J_a$ ,  $J_w$  and SRF with successive trial and error of ratings so that practical solutions for tunnel and cavern support and reinforcement were obtained. Figure 4 shows the first distribution of case records in 1974, while Figure 5 shows the solution arrived at after collection of a large number of additional case records by Grimstad. We coined NMT (Norwegian Method of Tunneling) in 1992 [4].

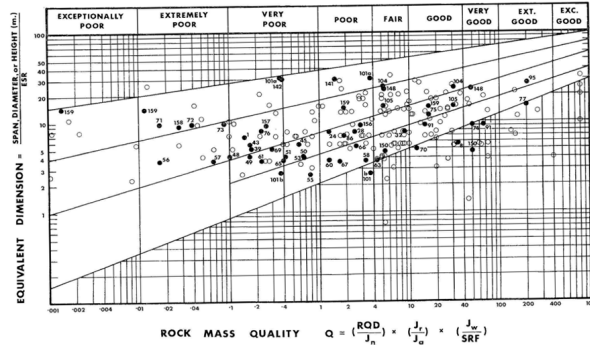


**Fig. 4.** The initial 212 case records for developing Q, saw some 60% from hydropower projects. The support selection scheme shown in Figure 5 was based on 1050 additional case records, mostly road tunnels that were logged by Grimstad, [5] see Grimstad and Barton, 1993.

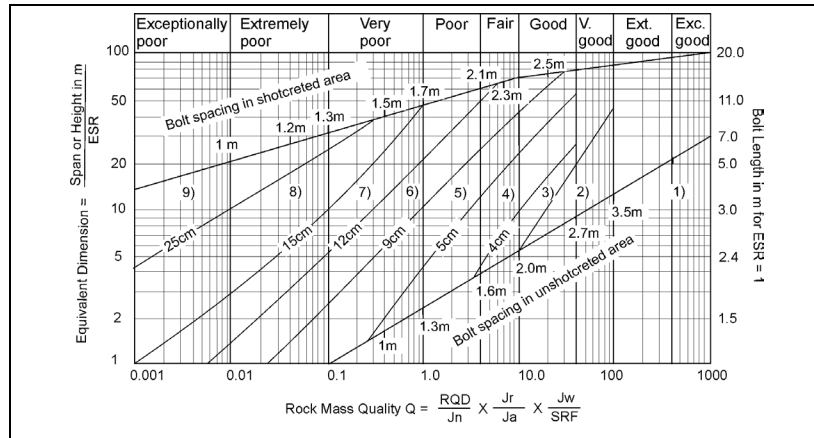
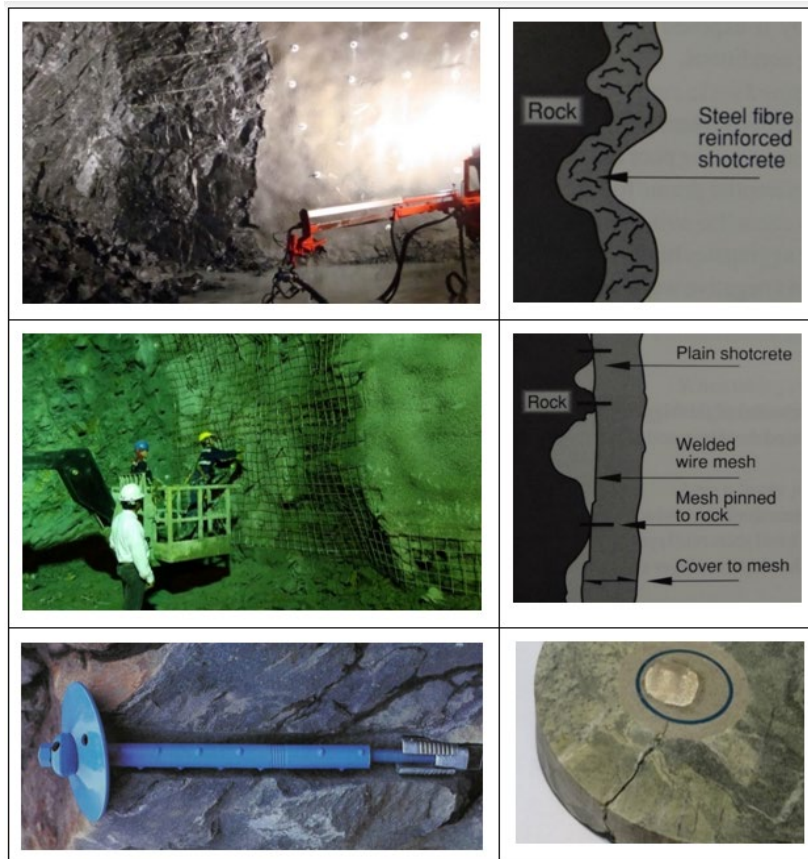


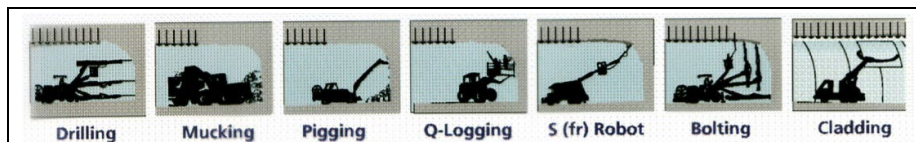
**Fig. 5.** The basic selection of rock bolt spacing (top diagonal) and thickness of fibre-reinforced shotcrete: steel 25-35kg/m<sup>3</sup> or PP 6 to 8kg/m<sup>3</sup>. When addressing RRS (rib-reinforced shotcrete arches) later, note slight S(fr) adjustments.

126 The huge advantages of fiber-reinforced shotcrete S(fr) as compared to the  
 127 older mesh-reinforced S(mr) are nicely illustrated in Figure 6, in the photo-  
 128 graphs of tunnel application and in realistic sketches by [6] Vandevall,1990.  
 129



130 **Fig. 6.** B + S(fr) is preferred to B + S(mr). CT-bolts (4 x corrosion protection  
 131 even after cracking of outer layer of grout) are important when single shell  
 132 B+S(fr) is the final support as in NMT. (Drawings from Vandevall, 1990).  
 133  
 134

135 The typical NMT operations are shown in Figure 7 and include Q-logging.  
 136



137 **Fig.7.** NMT single-shell operations may include PC-element cladding and  
 138 outer membrane. This is where traffic is heavier and good lighting is needed.



RRS (rib-reinforced shotcrete arches) shown in Figure 8 are much more robust than the lattice girders (LG) commonly used in NATM because they are radially bolted and have a 3D arching effect when closely spaced.

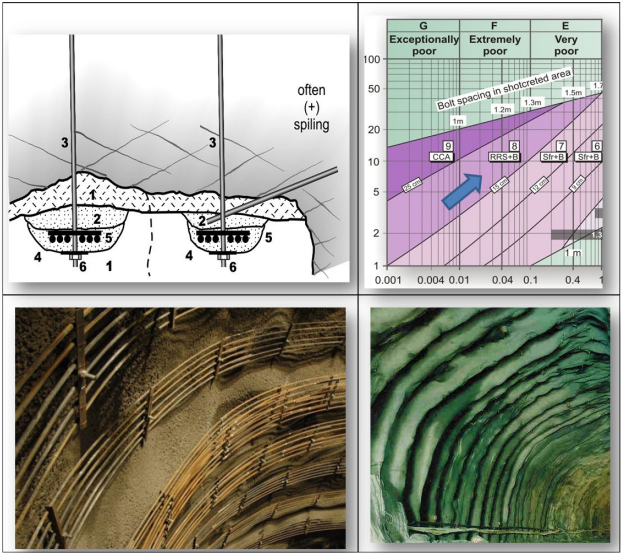


**Fig. 8.** The principles of RRS (rib-reinforced shotcrete) arches.

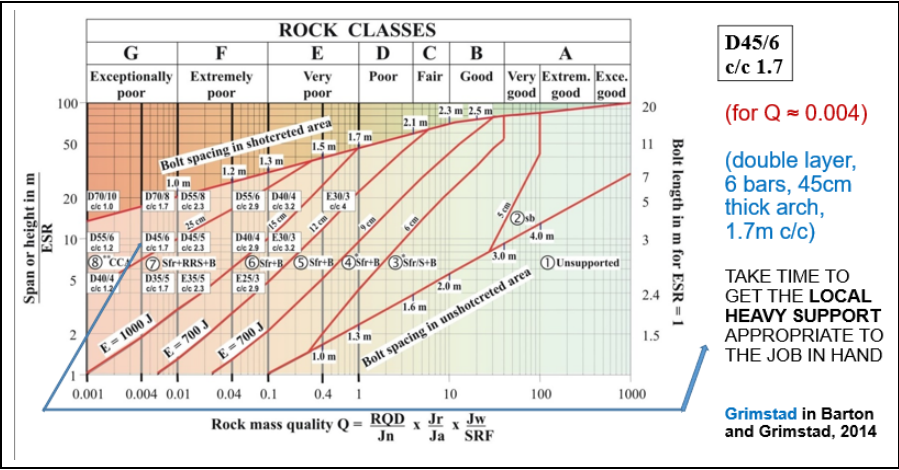


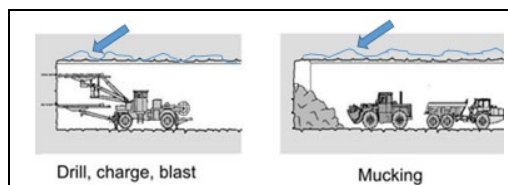
**Fig. 9.** Empirically based and partially numerically modelled by Grimstad's colleagues in NGI, this is the more complete set of RRS dimensioning compared to a truncated version in recent Road Authority sponsored NGI work. RRS have the advantage of no reliance on maybe deforming LG footings. See [7] Barton and Grimstad, 2014.

## 151 2.2 Double-shell NATM as an alternative to NMT

152 Because the Q-system was developed in Norway based on single-shell solu-  
 153 tions of B + S, S(mr) and finally S(fr) we had coined the letters NMT to con-  
 154 trast it from NATM. This was a multiple-company, multiple-author marketing  
 155 idea as we considered NMT sounder than NATM because of the temporary  
 156 support phase of NATM with its ‘soft’ lattice girders. These can fold when  
 157 over-loaded as we shall see. Figure 10 illustrates the main stages of NATM.  
 158



159 **Fig. 10.** NATM tunnel excavation stages from [8] ASG, 2010.

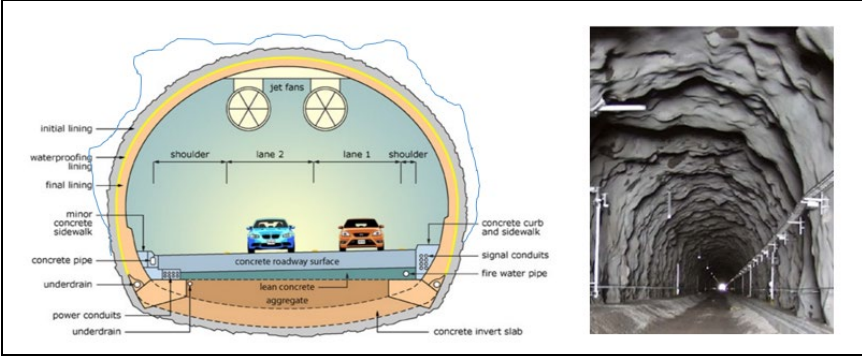


161 **Fig. 11.** Over-break may affect most stages of NATM-based construction.

162  
 163 Tunnel designers seldom or never include the possible over-break in their  
 164 convincing-looking designs. Nevertheless, structural geological details may  
 165 get in the way of such optimism, and contractors are then finding their shot-  
 166 crete (or concrete) volumes are sometimes far greater than expected. There  
 167 have been commercial arbitrations on such matters, and on occasion two Q-  
 168 parameters have been used to support contractor's claims, namely  $J_n/J_r$ . As  
 169 will be seen in Figures 12 and 13 overbreak can be expected and explained.



170

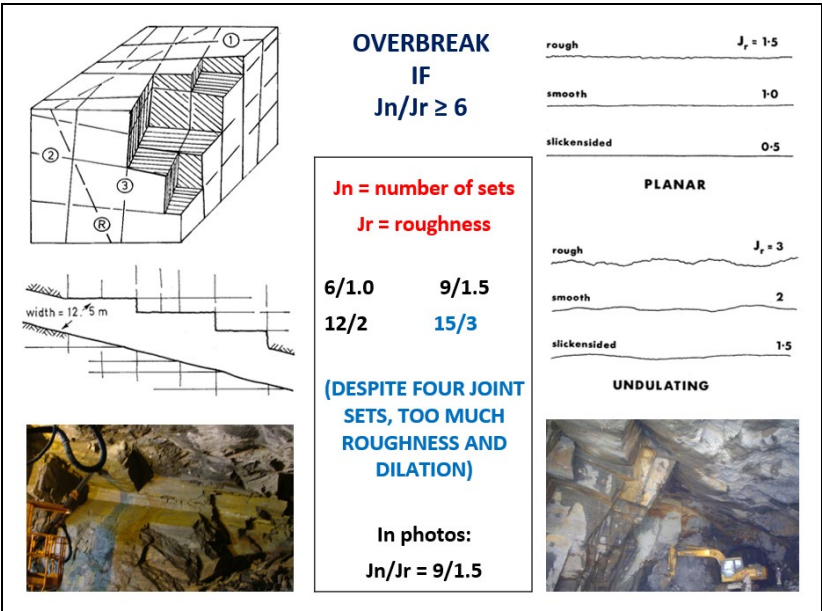


171 **Fig. 12.** An over-break ‘warning’ for NATM, while in NMT it is expected.

172 Overbreak depends not only on the care or lack of care with drill and blasting  
173 but also on the properties of the rock mass, in particular the degree of freedom  
174 for block formation and the all-important inter-block shear strength.

175 **2.3 Q-parameters of Special Importance in Tunnelling**

176 Figure 13 is a demonstration of why both  $J_n$  and  $J_r$  are important for the de-  
177 gree of over-break. Even with careful blasting it may be impossible to prevent  
178 over-break. It very much depends on the ratio of  $J_n$  and  $J_r$ . Ja ‘helps’ too.  
179



180 **Fig. 13.** Ratio of 2nd and 3rd Q-parameters. If  $J_n/J_r \geq 6$  overbreak is likely.

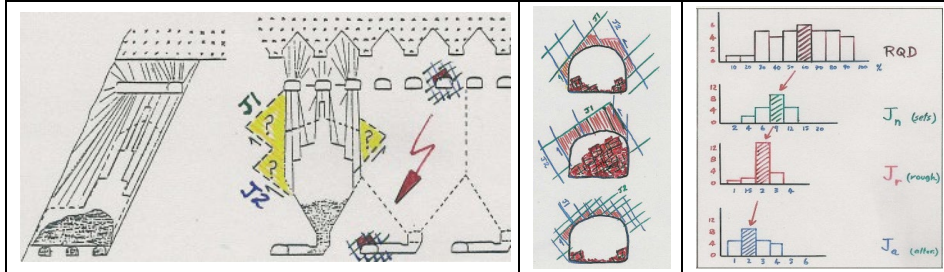


**Fig. 14.** Over-break in a mining (long-hole drilling) project in LKAB. Extreme-value Q-parameter statistics, helped by adverse  $J_a$  caused massive over-break, almost collapse in some of the drilling galleries, as sketched by NRB.

This mining case record resulting from a visit to the OSCAR project in LKAB, Sweden is a good example of the value of the fourth parameter ( $J_a$ ) in the Q-system: the ratio  $J_r/J_a$  is illustrated in Figure 15.

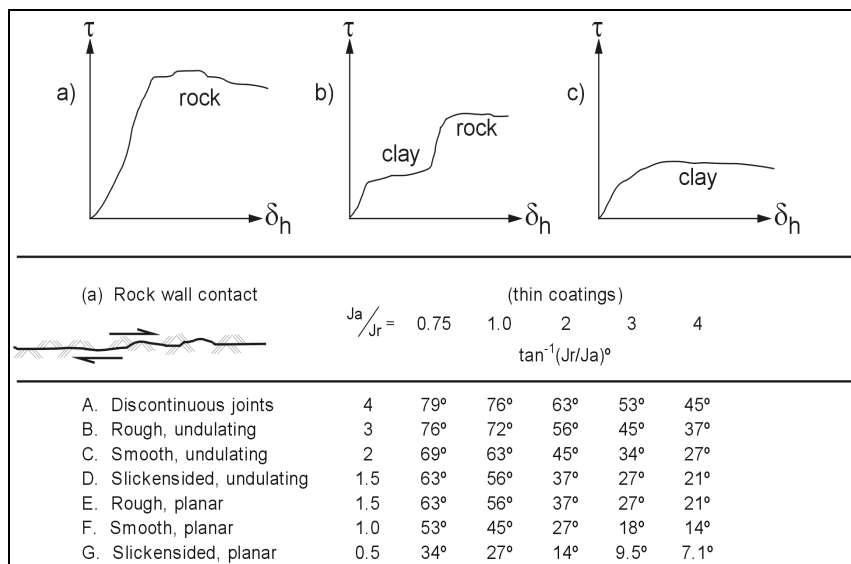


**Fig. 15.** The ratio  $J_r/J_a$  is a close approximation to friction coefficients. 'Dilation potential': additional ° if  $J_r$  is high. (' $\phi+i$ ' effect). 'Contraction potential' (subtraction of ° degrees if  $J_a$  is high. (' $\phi-i$ ' effect).

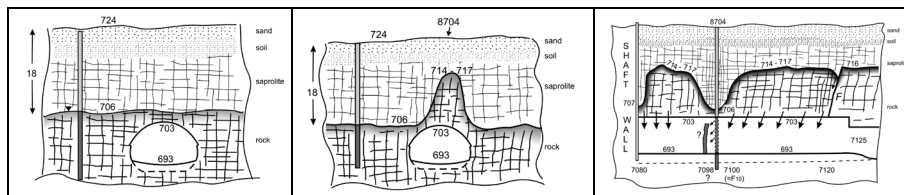
### 3 The Choice of Tunneling Method may have Consequences

Some years ago the author presented a paper in Hong Kong with the title: 'The Shallow Metro Syndrome'. This was in response to several years following a new metro line in São Paulo, Brazil: Linha 4-Amarela. Here, despite

197 warnings by several experts, the designers insisted on ‘short escalators’ per-  
 198 haps having concern for passengers’ experiences and future maintenance  
 199 costs. They failed to understand the time and cost consequences of mixed-face  
 200 tunneling through saprolite, clay, granite or gneiss, choosing the eleva-  
 201 tion/shallow depth where each could be met in the same tunnel face. The sta-  
 202 tion cavern 1km away in granite suffered 2 to 4m over-break. (Fig. 16). The  
 203 other end of the station was in clay. This had enormous consequences on cost  
 204 and delay and indirectly cost seven lives at the next station. Lattice girders  
 205 and shotcrete were overcome by the vertical loading from an unanticipated  
 206 10m high ridge of ‘differentially *unweathered*’ gneiss. It was not discovered  
 207 despite five nearby boreholes on either side of the planned station cavern, and  
 208 one on the axis of the future cavern. Figures 17 and 18 show consequences.  
 209



210 **Fig. 16.** Shallow metro consequences: mixed-face, overbreak, collapse?  
 211

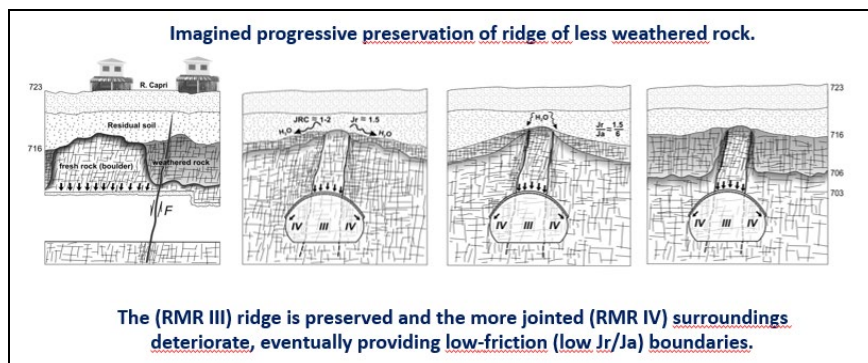


212 **Fig. 17.** Five boreholes surrounding or within the planned station cavern  
 213 failed to reveal the presence of a ridge-of-rock, which had a ‘fatal’ fracture  
 214 zone along its axis. All five boreholes suggested just 3m of rock cover. This  
 215 10m high ridge was the result of differential weathering. ‘Robust’ LG of  
 216 32mm x 25mm x 25mm folded, allowing the less weathered rock to fall 10m.

217 This caused the massive collapse seen in Figure 18. Five people driving in a  
 218 minibus died. Two pedestrians were also sucked into the collapse.  
 219



220 **Fig. 18.** The collapse of the Pinheiros Station cavern during construction. The  
 221 fatalities occurred along the small road (Rua Capri) seen on the right.  
 222



223 **Fig. 19.** Possible ‘morphologic’ representation of the historic progression of  
 224 differential weathering that caused 2007 over-loading of lattice girders at Pin-  
 225 heiros. Figure 21 illustrates why lattice girders need careful consideration.  
 226



227 **Fig. 20.** This shows part of the loosened ‘ridge-of-rock’ after it fell 10m.





**Fig. 21.** Before and after. Lattice girders of 32mm x 25mm x 25mm capacity appear to have limited strength when confronted with a large concentrated vertical load. Designers are usually assuming a rare evenly distributed load.

On another occasion contractors tunneling for a motorway city bypass through presumed jointed granites had to tackle deeply weathered (saprolitic) materials at each end. So in principle NATM solutions were chosen for the first 150-200m at each end of the tunnel, and NMT-style Q-based B + S(fr) in the central hard rock kilometers in jointed granite. The over-simplified design for the 'NATM' sections is illustrated in Figure 22. Regrettably both the sloping ground (inexcusable) and vertically oriented phyllite and a dike (not discovered) were not modelled. Approximately 140m of the right tube collapsed on a Saturday afternoon when all the tunnelers were at a God-given barbeque. Three months later the parallel tube also collapsed. There were no casualties as the site was closed pending a hearing. Collapse model by Bandis, Fig. 23.

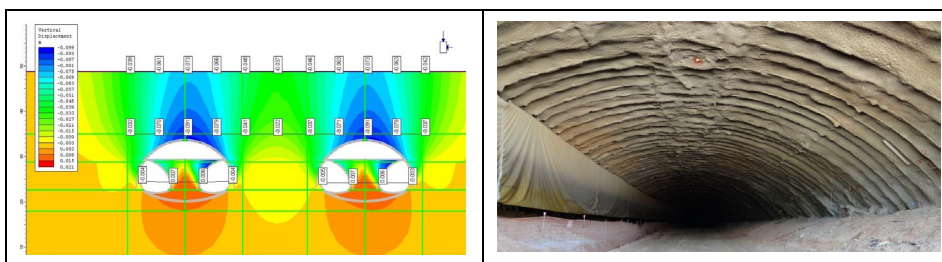


**Fig. 22.** Optimistic symmetric design, when actually sloping ground. Light lattice girders. No bolts due to saprolite. Much more than specified shotcrete thickness due to 30 to 80cm over-break. This is the second tube. 140m collapsed three months after the 1<sup>st</sup> 140m collapse. Again, lattice girders folded.



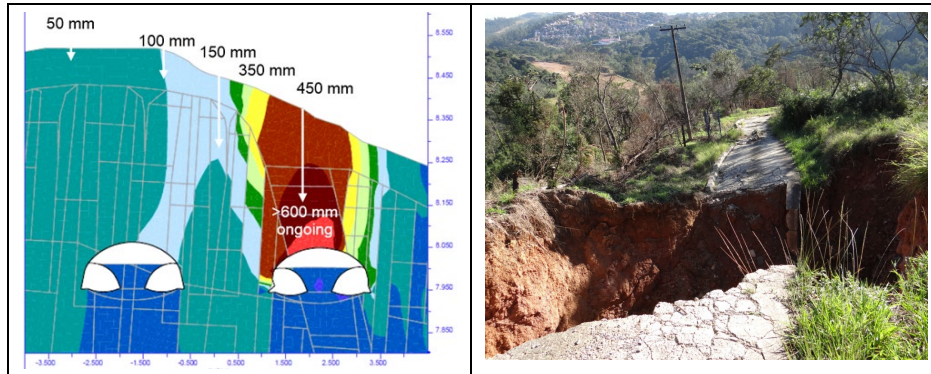


**Fig. 23.** When the vertical structure (and sloping ground) was modelled the imminent failure is understood. The photograph is after the 2<sup>nd</sup> tube collapse.

Why lattice girders are prone to collapse is suggested in Figure 24. Firstly, reinforcing any rock mass with systematic bolting and holding it in place with shotcrete (solving the frictional strength/weakness and cohesive strength/weakness) is obviously positive, as proved by the experimental tunnel results (left), which show how poorly steel sets are working. (Deformation and loosening and maybe loss of strength is needed).

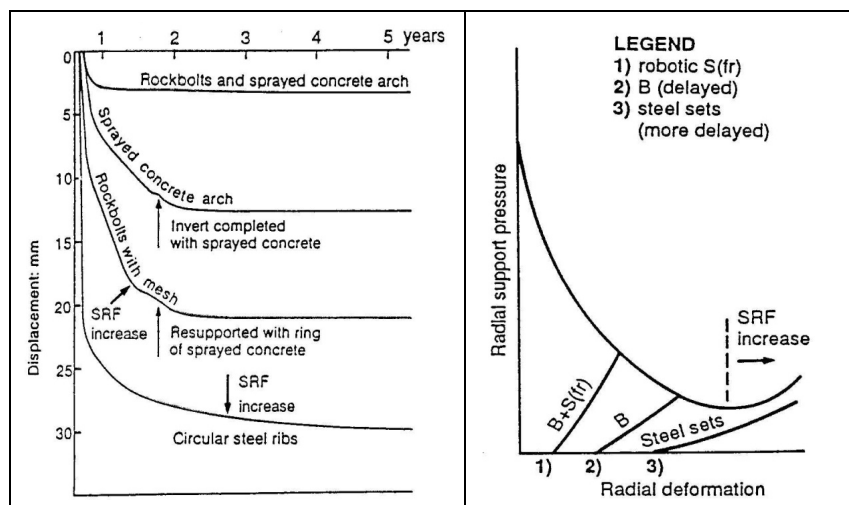
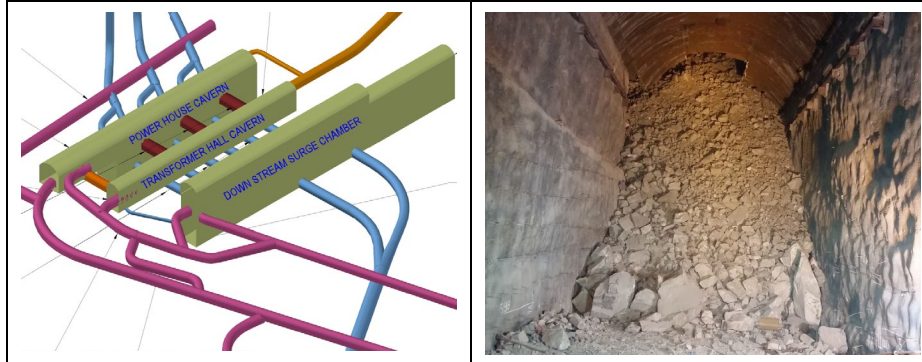


**Fig. 24.** Left: Avoidance of steel sets (or lattice girders) remains an important advisory for NMT Q-system users. The instrumented experimental tunnel was driven in mudstones. [9] Ward et al. 1983. Right: Steel sets and lattice girders allow and even require loosening of the rock mass to make better contact, i.e. an increase of SRF in the Q-value. [10] Barton and Grimstad, 1994. The use of steel sets with constant spacing so not allowing for faulted rock, i.e. increased loading, can cause tragic collapses (see Figures 25, 26).



265 **Fig. 25.** Collapse in partly completed down-stream surge chamber arch in an  
 266 Asian country. Tragically, six workers were caught in the collapse. First collapse  $\approx$   
 267 35,000 m<sup>3</sup>. It is not known if an unseen progressive failure had been occurring.



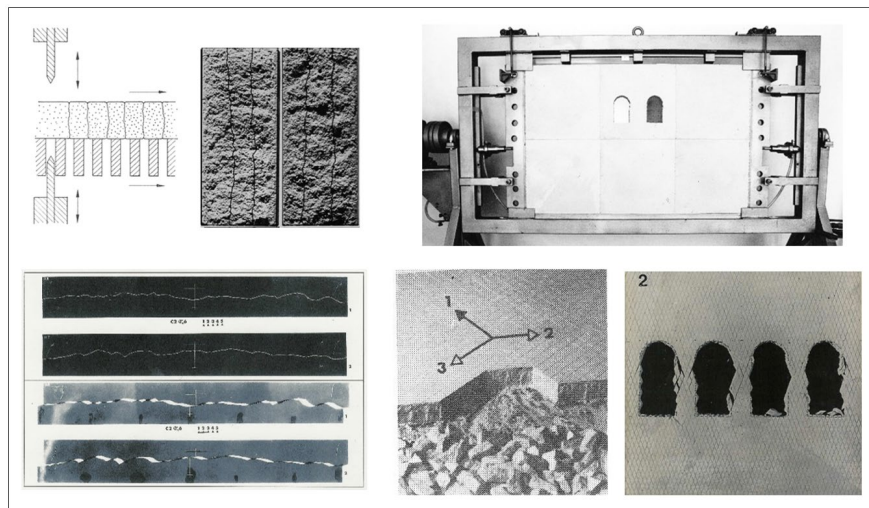
268 **Fig. 26.** There was an attempt to remove fallen rock (approx. 15,000 m<sup>3</sup> was  
 269 removed). Note the extra destruction of steel sets in the 'left' arch due to the  
 270 fault. A larger collapse subsequently occurred, shown on the right.

271  
 272 The total volume of collapsed rock mass was by now approx. 70,000m<sup>3</sup>, basi-  
 273 cally initiated due to constant steel set spacing despite changed conditions. As  
 274 a point of difference when using NMT there is a specific 'owner's half-hour'  
 275 when engineering geologists representing both sides (owner, contractor) map  
 276 conditions together and try to agree on the Q-based 'support class'. This oc-  
 277 curs after every blast. (It is part of the cycle-time and is seen in Figure 7  
 278 which was first published more than 30 years ago). Care is needed in tunnels.  
 279

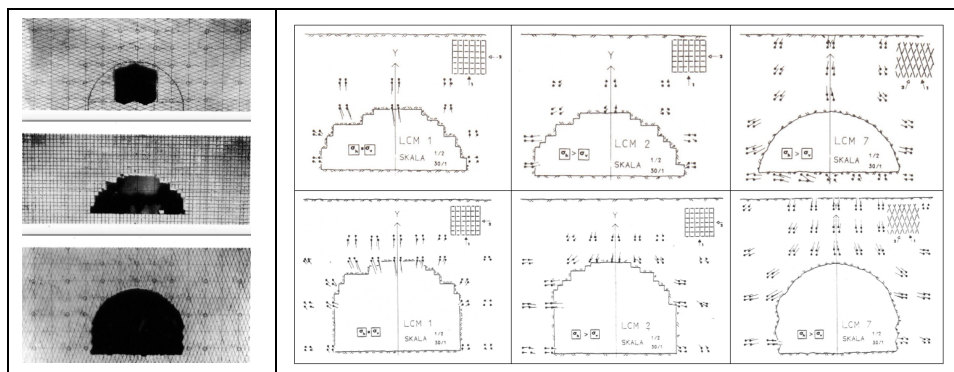
#### 280 **4 A Glimpse of Physical and Numerical Modelling with Joints**

281 In this section the 62m span Gjøvik Olympic cavern will be illustrated as it is  
 282 a good example of efficient construction and (NMT) economic support. It was  
 283 constructed for the 1994 Winter Olympics. The idea to build an underground

284 ice rink came from Consulting Engineer Jan A. Rygh, who was visiting his  
 285 company's underground swimming pool. While having dinner with Gjøvik's  
 286 Municipal Engineer in 1988, he was informed of the news that Gjøvik had  
 287 been awarded an ice rink for the Olympics. The first drafts were sketched on a  
 288 napkin in the restaurant. Ten years before this the present author had been  
 289 busy with physical models of 50m span caverns for possible underground  
 290 nuclear power plants. This was research work at NGI sponsored by Norway  
 291 and Sweden (BeFo). Figure 27 shows the approach used and Figure 28 some  
 292 results of the deformations. A brittle model material, a double-bladed guil-  
 293 lotine, and photogrammetric recording of deformations were the essential com-  
 294 ponents, besides the rotatable loading frame for applying gravity and horizon-  
 295 tal stresses. Ten years later, Figs. 29 and 30, a real and even larger cavern.  
 296



297  
 298 **Fig. 27.** Physical modelling method with rough interlocked fractures.  
 299



300 **Fig. 28.** Examples of the large span caverns. Note the strong effect of joint  
 301 orientations and whether applying isotropic stress or tectonic horizontal stress.



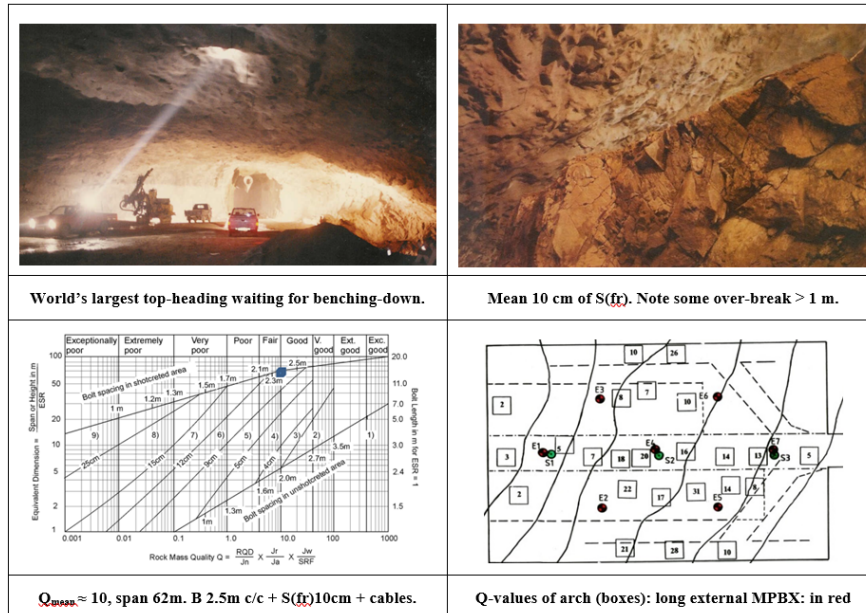


**Fig. 29.** The 62m span Gjøvik Olympic cavern.  $Q_{mean}$  of approx. 10 needed 10cm of S(fr) (Dramix steel fibre) + 2.5m c/c corrosion-protected CT bolts.

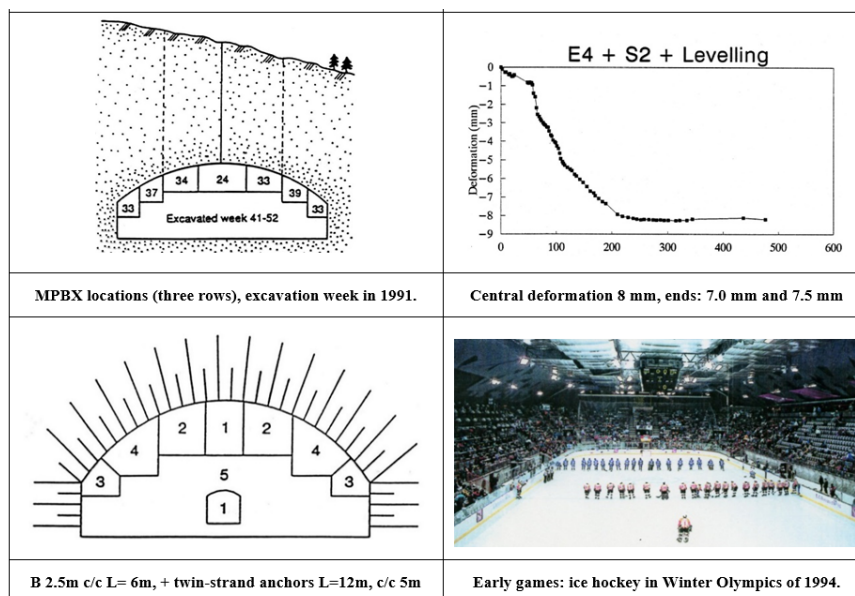


**Fig. 30.** Seven MPBX extensometers from the surface showed maximum 8mm deformation. This was very close to the predicted deformations resulting from prior UDEC-BB modelling. The modelling (Figures 31, 32, 33) is a demonstration of how much is lost by those performing continuum models.



**Fig. 31.** Scoping studies with UDEC-BB show the positive effect of higher horizontal stress. With continuum modelling such improvement is in doubt.

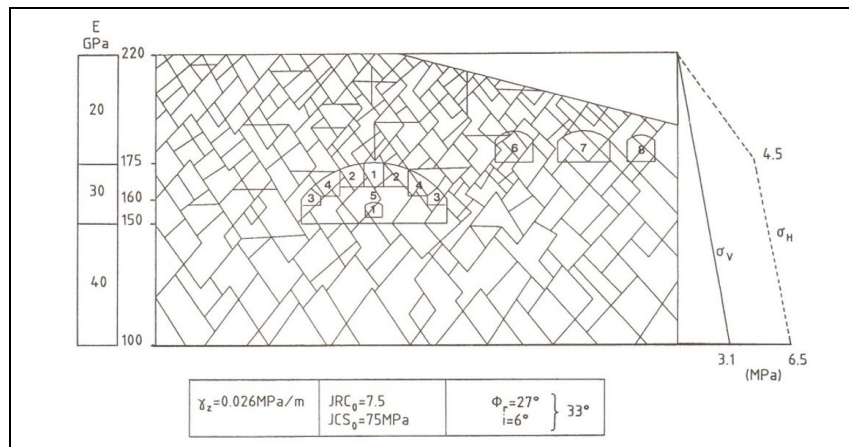


**Fig. 32.** The final UDEC-BB joint geometry for the cavern modelling, also showing the basic input data for the BB-criterion: JRC, JCS,  $\Phi_r$ . A 'Patton i-value' ( $6^\circ$ ) was added to make some allowance for large-scale joint undulation. Note the high horizontal stress, and depth-dependent deformation moduli. The latter reality is ignored in the Rocscience-GSI-H-B modelling. Many colleagues at NGI contributed to the 1994 paper: see [11] Barton et al. 1994.



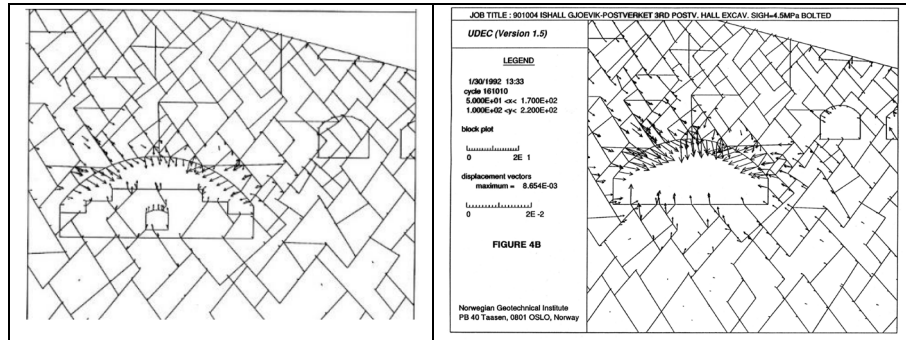


**Fig. 33.** Left: Modelling of the very large top-heading (seen in Figure 29). Right: Full-stage excavation (max. 8.7mm deformation) with a slight increase caused by Post Service caverns (one of 20m span) closer to the surface.

A notable result: our cross-hole tomography recorded increased  $V_P$  with depth, yet no RQD, nor  $F^{-1}$  nor Q-value increases with depth. Joints are simply more tightly closed at depth. Figure 34 shows two results. They correspond with the  $Q_c - V_P$  - depth method proposed in [12] Barton, 1995. See Figure 35.

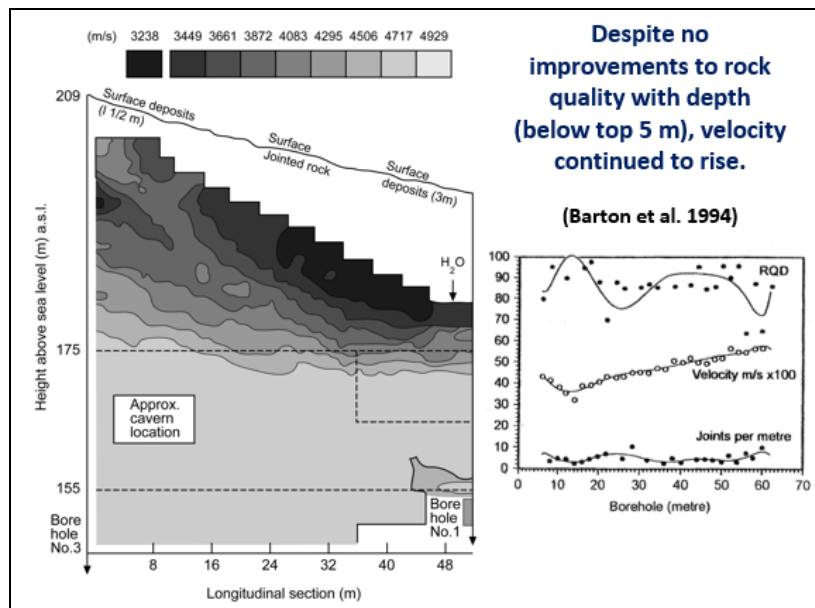
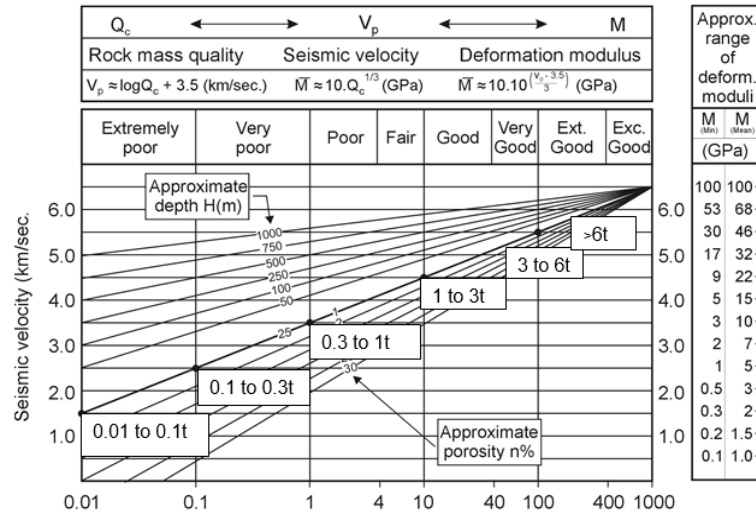


**Fig. 34.** Stress increase alone causes P-wave velocity to rise. This is shown in the plot of RQD and joints per meter spacing. The logged Q-value down this borehole also did not increase. Other results like this are found in the literature. A big review linking seismic qualities with rock qualities was given in [13] Barton, 2006. It is clear that velocity, and therefore deformation modulus must increase with depth, yet this is ignored by most numerical modelers.



$$Q_c = \left[ \frac{RQD}{J_n} \times \frac{J_r}{J_a} \times \frac{J_w}{SRF} \right] \frac{\sigma_c}{100}$$

**Fig. 35.** An empirically derived scheme linking Q<sub>c</sub> and V<sub>p</sub> with depth (+ve) and porosity (-ve). Recently the very approximate block size has been added based on observations. Beyond Q<sub>c</sub> of 50 to 100, blasting will be needed to produce desired block size ranges e.g. for marine structures: Figure 36.



**Fig. 36.** Block-size estimation using Q<sub>c</sub> and V<sub>p</sub> and vizual observation.

#### 4 Rock Slope Stability from a non-GSI Discontinuum Perspective

It was noted at the beginning of this paper that while the use of the Q-system dominates internationally for use in underground civil and mining, it is Evert Hoek's GSI (with influence from Paul Marinos) and Hoek and Brown's H-B equations that dominate concerning application for rock slopes. This is actually illogical as slopes are even more jointed than at depth in the rock mass. Yet joints and faults as discrete structural geology realities are ignored in the 'con-

tinuum camp'. The simplicity of GSI and the cheaper computer programs and faster 'results' are presumably the chief attractions of using potentially unreliable methods. This opinion is partly held due to participation in an international court case some years ago, in which the GSI-H-B Phase 2 modelling package was shown to grossly exaggerate so-called plastic zones. The predicted plastic EDZ of 10m to 14m horizontal dimension were for a small headrace tunnel driven 7km without needing shotcrete. It had suffered some invert damage, but only when emptied too fast (20m/hour or more) due to penstock worries.

The other reason for the 'unreliable methods' opinion is because so many are using 'the continuum package' to produce impossible circular failures when supposedly modelling slopes in jointed rock, with UCS even as high as almost 80MPa in the case of [14] Carranza-Torres, 2021. This inappropriate GSI and H-B application is shown in Figure 38.

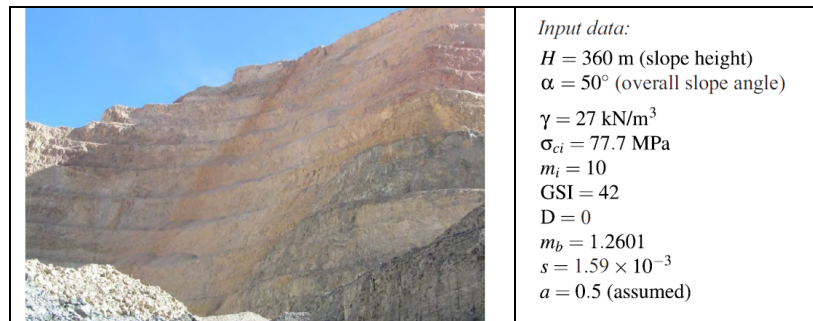
One problem with H-B based modelling is that not even the classic Mohr-Coulomb (M-C) equation involving the cohesive and frictional strength is correct, since rock masses fail (if unstable enough) by a progressive mechanism. So whether linear (M-C) or non-linear (H-B) it is actually not correct to add, as if instantaneous 'c' plus ' $\sigma_n \tan \phi$ '. Cohesion weakening and friction hardening (CWFH) or 'c' then ' $\sigma_n \tan \phi$ ' follows real events in rock masses more closely than using the '+' sign. An even better solution is shown later.

Few of the users of GSI and H-B seem to be aware of the multiple repetition of GSI in the H-B equations for the roughly estimated 'c' and ' $\phi$ '. The two page-wide equations are reproduced in Figure 37 in yellow and green. Three of the supporting equations for  $m_b$ , s and a are also shown. They prompted Barton, 2025 [15] to suggest that GSI is repeated respectively 16 and 12 times in the main H-B equations. This seemed to be a record, but no.

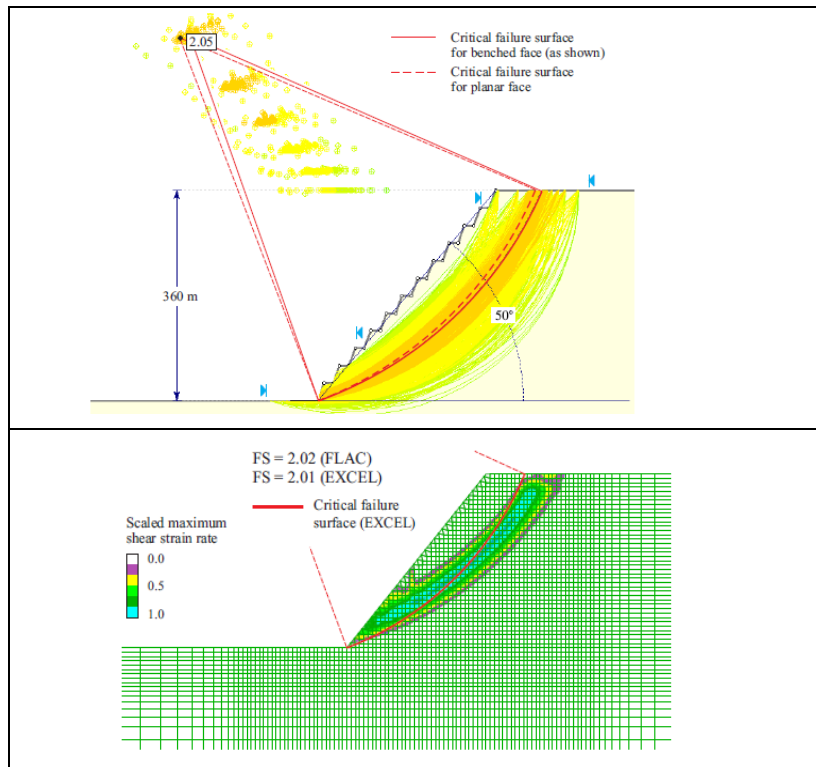
$c' = \frac{\sigma_{ci} [(1+2a)s + (1-a)m_b \sigma'_{3n}] (s + m_b \sigma'_{3n})^{a-1}}{(1+a)(2+a) \sqrt{1 + (6am_b(s + m_b \sigma'_{3n})^{a-1}) / (1+a)(2+a)}}$	
$\phi' = \sin^{-1} \left[ \frac{6am_b(s + m_b \sigma'_{3n})^{a-1}}{2(1+a)(2+a) + 6am_b(s + m_b \sigma'_{3n})^{a-1}} \right]$	
$m_b = m_i \exp\left(\frac{GSI-100}{28-14D}\right)$	$s = \exp\left(\frac{GSI-100}{9-3D}\right)$
$a = \frac{1}{2} + \frac{1}{6} \left( e^{-\frac{GSI}{15}} - e^{-\frac{20}{3}} \right)$	
$\sigma'_{c,m} = \sigma_{ci} \frac{[m_b + 4s - a(m_b - 8s)](m_b / 4 + s)^{a-1}}{2(1+a)(2+a)}$	$E_m (\text{MPa}) = 10^5 \left( \frac{1 - D/2}{1 + e^{\left[ \frac{75 + 25D - GSI}{11} \right]}} \right)$

**Fig. 37.** GSI is repeated many times in these H-B estimates of rock mass 'c' and ' $\phi$ ' and  $\sigma'_{cm}$ . In fact a fourth supporting equation has been omitted so far.

381 If the H-B equation for  $\sigma'_{3n}$  is also included, the 16-times repetition of GSI for  
 382 'c' has to be increased to 16+10+10+10 = 46-times (!), and the 12-times repe-  
 383 tition for 'φ' has to be increased to 12+10+10 = 32-times (!). This means 78-  
 384 times repetition of GSI in a supposed equation for the shear strength of rock  
 385 masses. Remarkably, thousands of users of Rocscience software are presuma-  
 386 bly unaware of these fundamentally unreliable GSI/H-B methods. If the B-B  
 387 equation given by Barton, 1973 [16] had JRC and JCS repeated *even twice* it  
 388 would be unknown in rock mechanics. The GSI situation is not scientific.  
 389



390

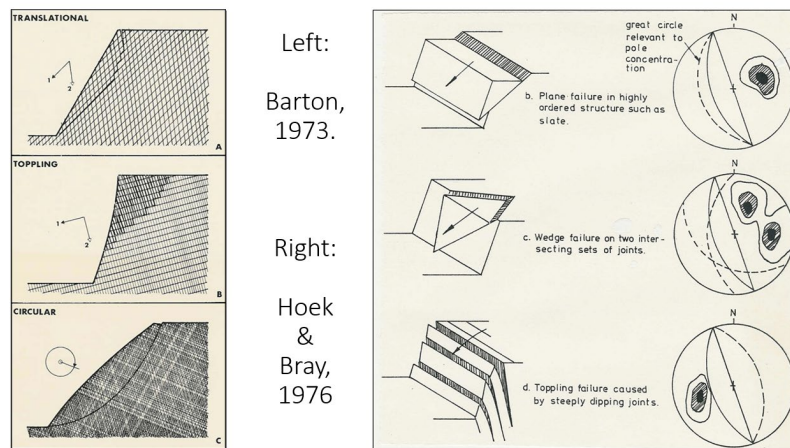


391 **Fig. 38.** GSI + H-B predictions for an open pit with UCS = 77.7MPa. [14].



392 We may also note that even the intact rock and genuinely empirical Hoek-  
 393 Brown equation has insufficient curvature if confining pressure is increased.  
 394 This was demonstrated in a comprehensive review of high stress (mining rel-  
 395 evant) triaxial data by [17] Singh et al. 2012, and also by [18] Shen et al.  
 396 2021. It means that the intact rock H-B criterion is non-conservative in deep  
 397 mines. This aspect will be shown at the end of this paper.

398 Leaving GSI and its unfortunate 78-times repetition in so many people's  
 399 models, we can take a look at idealized but realistic drawings of jointed rock  
 400 masses as they affect rock slopes. We can start with an historic Hoek and  
 401 Bray, 1976 [19] trio of drawings with analysis method (right) and three larger-  
 402 scale sketches from an earlier student at Imperial College (left).  
 403



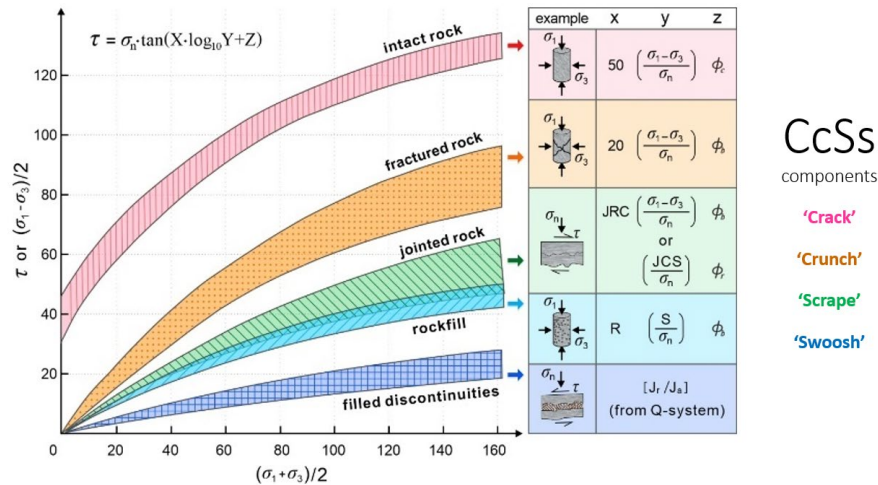
404  
 405 **Fig. 39.** Six sketches of rock slopes at different scales. [16], [19]. These repre-  
 406 sent simplifications of reality. Circular failures such as in Figure 38 are not  
 407 reality unless the slopes are in very weak rock, saprolite or rockfill.  
 408



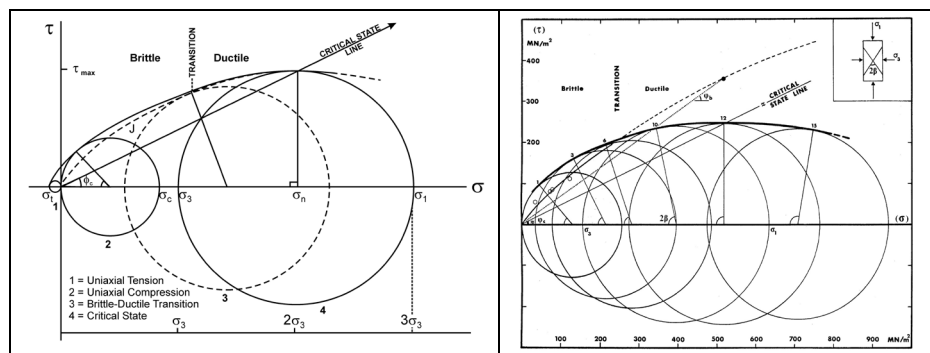
409 **Fig. 40.** A dramatic and record 70,000,000m<sup>3</sup> failure at Bingham Canyon  
 410 Mine in Utah. It measures 3km from crest to run-out toe. Some might assume  
 411 'circular' failure, but a 300-400m long fault plane was involved.



412 Progressive failure was involved in the large failure shown in Figure 40. The  
 413 common ability to monitor slopes and withdraw equipment and personell is  
 414 important for the open-pit mining industry. Big slopes do not fail during ‘the  
 415 click-of-a-finger (the ‘+’ sign in linear M-C and in the non-linear GSI-infested  
 416 H-B). The scheme shown in Figure 41 may offer a solution.  
 417

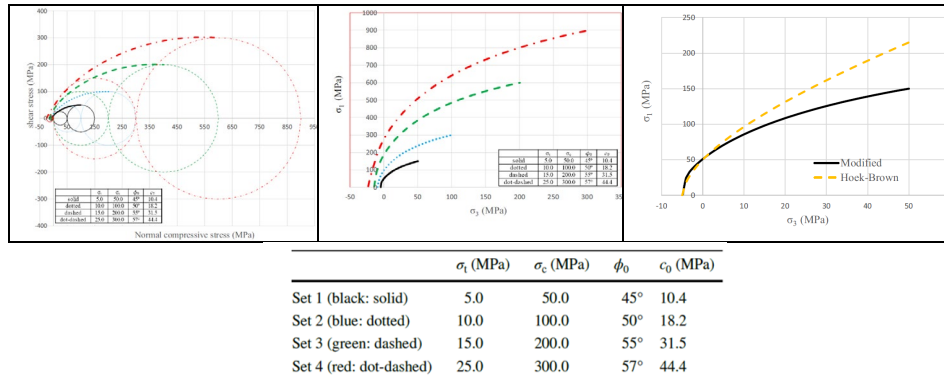


418  
 419 **Fig. 41.** A progressive failure suggestion: intact rock bridges with cohesive  
 420 strength may need to fail first ('crack' = C). The rough, fresh fracture surfaces  
 421 are immediately sheared ('crunch' = c). Kinematically capable joints or joint  
 422 set(s) may then be mobilized in the potentially growing progressive failure  
 423 ('scrape' = S). Quite often it seems that major fault planes that perhaps are  
 424 water saturated are involved, for instance completing a wedge ('swoosh = s).  
 425 Each of the above CcSs are roughly quantified (see x, y, z): [20] Barton, 1999.  
 426 Regarding the shear strength of intact rock (the 'C' in CcSs), note Figure 42.  
 427



428 **Fig. 42.** A basically simple intact rock shear strength criterion is shown (left)  
 429 based on the critical state suggestion of [21] Barton, 1976.

430 In Figure 42 the uniaxial Mohr circle almost touches the critical state confin-  
 431 ing pressure  $\sigma_3$ . The set of experimental triaxial data for a strong limestone  
 432 demonstrates that circles 1 and 12 are even closer. Singh et al. 2011 [17]  
 433 showed that this is typical for most rock types. As a curiosity, the diameter of  
 434 the UCS Mohr circle is equal to the critical state maximum shear strength (the  
 435 radius of the largest Mohr circle (Figure 42, left). This ‘simplicity’ can actual-  
 436 ly explain maximum mountain heights of about 9km. This is another story.  
 437



438  
 439 **Fig. 43.** Two simple sets of shear strength equations were developed by [22]  
 440 Shen et a. 2018 to match with the Barton critical state suggestion. Four sets of  
 441 input data and resulting  $\phi$  and  $c$  are shown in this figure. The inadequate cur-  
 442 vature of the intact rock H-B equation at high stress is also shown, similar to  
 443 the same discrepancy demonstrated earlier by [17] Singh et al. 2011.

## 444 5 Conclusions

- 445 1. The gradually developed popularity of the Q-system for use in under-  
 446 ground tunnelling and mining, and the added use of the ratio  $J_n/J_r \geq 6$   
 447 to explain overbreak is boosted by use of the ratio  $J_r/J_a$  to quantify an  
 448 approximate friction coefficient. This can be useful for conservative  
 449 estimates of the frictional strength of filled discontinuities and the po-  
 450 tential weakness of faults with clay cores.
- 451 2. When using the Q-system for tunnel periphery reinforcement and sup-  
 452 port using single-shell B + S(fr), what we term NMT, we have the  
 453 additional RRS if needed. This is a much more robust bolted structure  
 454 than the unbolted lattice girders used in typical double-shell NATM.
- 455 3. Lattice girders need rock mass deformation to function because longi-  
 456 tudinal strain must precede radial support capabilities. Some notable  
 457 collapses of LG or steel sets during construction were illustrated.
- 458 4. Due to a background in physical models of slopes and caverns in  
 459 jointed (tension fractured) brittle materials, and the general observa-

460 tion of the ubiquitous nature of jointing and sometimes faulting in  
 461 hundreds of projects world-wide, plus a life-long emphasis on discon-  
 462 tinuum description (JRC, JCS, Jr, Ja) such quantification and its use  
 463 in modelling has appeared as obviously preferable to unrealistic con-  
 464 tinuum modelling.

- 465 5. The current trend for GSI and Hoek-Brown based continuum model-  
 466 ling for slopes, and the frequent publication of impossible circular  
 467 failure modes even in competent jointed rock, has alerted some of us  
 468 to question the strangely fabricated H-B equations.
- 469 6. Due to four supporting equations including those for  $m_b$ ,  $s$  and  $a$ , one  
 470 finds that GSI appears an incredible 78-times in the H-B equation for  
 471 the supposed non-linear shear strength of rock masses. This is inde-  
 472 fensible yet is used by thousands who do not see the reality due to  
 473 convenient Rocscience input-data software and fast modelling results.
- 474 7. Rock masses have several components of shear strength and potential  
 475 weakness. Mohr-Coulomb and Hoek-Brown additions of 'c' and  $\sigma_n$   
 476  $\tan \phi$  need replacement with CWFH or with four-components CcSs.
- 477 8. A critical state shear strength suggestion of 50 years vintage sees UCS  
 478 Mohr circles approximately touching (tangential) the maximum shear  
 479 strength Mohr circle at the highest confining pressure needed to reach  
 480 the critical state. This convenient and well researched result also  
 481 shows that the Hoek-Brown intact rock strength criterion is insuffi-  
 482 ciently curved, so is non-conservative in the deep mining context.

## 483 6 References

- 484 1. Barton, N. & Choubey, V. The shear strength of rock joints in theory and  
 485 practice. Rock Mechanics 1/2:1-54. Vienna: Springer. (1977).
- 486 2. Bandis, S., Lumsden, A. & Barton, N. Experimental studies of scale ef-  
 487 fects on the shear behaviour of rock joints. Int. J. of Rock Mech. Min. Sci.  
 488 and Geomech. Abstr. 18, 1-21 (1981).
- 489 3. Erharter, G. H., N. Bar, T. F. Hansen, S. Jain and T. Marcher. International  
 490 Distribution and Development of Rock Mass Classification: A Review.  
 491 Rock Mechanics and Rock Engineering, [https://doi.org/10.1007/s00603-](https://doi.org/10.1007/s00603-024-04215-8)  
 492 024-04215-8 (2024).
- 493 4. Barton, N., Grimstad, E., Aas, G., Opsahl, O.A., Bakken, A., Pedersen, L.  
 494 & Johansen, E.D. Norwegian Method of Tunnelling. WT Focus on Nor-  
 495 way, World Tunnelling, June: 6p. August: 5p (1992).
- 496 5. Grimstad, E. & Barton, N. Updating of the Q-System for NMT. Proceed-  
 497 ings of the International Symposium on Sprayed Concrete - Modern Use  
 498 of Wet Mix Sprayed Concrete for Underground Support, Fagernes, 1993,  
 499 Norwegian Concrete Association, Oslo, pp. 46-66.

- 500 6. Vandevall, M. Dramix - Tunnelling the World. NV Bækert S.A, (1990).
- 501 7. Barton, N. and E. Grimstad. Q-system - an illustrated guide following forty years in tunnelling. Web site [www.nickbarton.com](http://www.nickbarton.com) 43p. (2014).
- 502
- 503 8. Austrian Society for Geomechanics: NATM: The Austrian Practice of
- 504 Conventional Tunneling. (2010).
- 505 9. Ward, W.H., Todd, P. and Berry, N.S.M: The Kielder Experimental Tunnel: Final Results. *Geotechnique* 33, 3, pp. 275-291 (1983).
- 506
- 507 10. Barton, N. & Grimstad, E: The Q-system following twenty years of application in NMT support selection. 43rd Geomechanic Colloquy, Salzburg.
- 508 Felsbau, 6/94. pp. 428-436 (1994).
- 509
- 510 11. Barton, N., By, T.L., Chryssanthakis, P., Tunbridge, L., Kristiansen, J.,
- 511 Løset, F., Bhasin, R.K., Westerdahl, H. & Vik, G. Predicted and measured
- 512 performance of the 62m span Norwegian Olympic Ice Hockey Cavern at
- 513 Gjøvik. *Int. J. Rock Mech, Min. Sci. & Geomech. Abstr.* 31:6: 617-641.
- 514 Pergamon. (1994).
- 515 12. Barton, N. The influence of joint properties in modelling jointed rock
- 516 masses. Keynote Lecture, 8th ISRM Congress, Tokyo, 3: 1023-1032,
- 517 Balkema, Rotterdam. (1995).
- 518 13. Barton, N. *Rock Quality, Seismic Velocity, Attenuation and Anisotropy*.
- 519 Taylor & Francis, UK & Netherlands, 729 p. (2006).
- 520 14. Carranza-Torres, C. Computational tools for the analysis of circular failure of rock slopes. Keynote, EUROCK 2021, Torino, Italy. (2021).
- 521
- 522 15. Barton, N. 2025. Twenty Strange Years in the World of Rock Mechanics and Engineering Geology. *Current Trends in Civil & Structural Engineering*, ISSN: 2643-6876 DOI: 10.33552/CTCSE.2025.11.000768
- 523
- 524
- 525 16. Barton, N: Review of a new shear strength criterion for rock joints, *Engineering Geology*, Elsevier, Amsterdam, Vol. 7, pp. 287-332. (1973).
- 526
- 527 17. Singh, M., Raj, A. and B. Singh: Modified Mohr-Coulomb criterion for non-linear triaxial and polyaxial strength of intact rocks. *Int. J. Rock Mech. Mining Sci.*, 48(4), 546-555 (2011).
- 528
- 529
- 530 18. Shen, B., J. Shi & N. Barton: Graphic Examples of a Logical Nonlinear Strength Criterion for Intact Rock. *Rock Mech Rock Eng* (2020) 53:71-75 DOI 10.1007/s00603-019-01902-9 (2020).
- 531
- 532
- 533 19. Hoek, E. and J.H. Bray. *Rock Slope Engineering*. Inst. of Mining, London. (1976).
- 534
- 535 20. Barton, N. General report concerning some 20th Century lessons and 21st Century challenges in applied rock mechanics, safety and control of the environment. 9th ISRM Congress, Paris, 3: 1659-1679, Balkema, (1999).
- 536
- 537
- 538 21. Barton, N. The shear strength of rock and rock joints. *Int. Jour. Rock Mech. Min. Sci. and Geomech. Abstr.*, Vol. 13, No. 9: 255-279. (1976).
- 539
- 540 22. Shen, B., Shi, J. & N. Barton. An Approximate Non-Linear Modified Mohr-Coulomb Shear Strength Criterion with Critical State for Intact Rocks. *Journal of Rock Mech. and Geotech. Eng.* 10, 645-652. (2018).
- 541
- 542